Published as: *Science*. 2021 March 26; 371(6536): 1350–1355.

Molecular mechanism of cytokinin-activated cell division in *Arabidopsis*

Weibing Yang[1,#], **Sandra Cortijo**[1,†], **Niklas Korsbo**[1], **Pawel Roszak**[1], **Katharina Schiessl**[1], **Aram Gurzadyan**[1], **Raymond Wightman**[1], **Henrik Jönsson**[1,*], **Elliot Meyerowitz**[1,2,*]

[1]Sainsbury Laboratory, University of Cambridge, Bateman Street, Cambridge, CB2 1LR, UK.

[2]Howard Hughes Medical Institute and Division of Biology and Biological Engineering, California Institute of Technology, 1200 East California Boulevard, Pasadena, CA 91125, USA.

Abstract

Mitogens trigger cell division in animals. In plants, cytokinins, a group of phytohormones derived from adenine, stimulate cell proliferation. Cytokinin signalling is initiated by membrane-associated histidine kinase receptors and transduced through a phosphorelay system. Here we show, in the Arabidopsis shoot apical meristem (SAM), that cytokinin regulates cell division by promoting nuclear shuttling of Myb-domain protein 3R4 (MYB3R4), a transcription factor that activates mitotic gene expression. Newly synthesized MYB3R4 protein resides predominantly in the cytoplasm. At the G2/M transition, rapid nuclear accumulation of MYB3R4—consistent with an associated transient peak in cytokinin concentration—feeds a positive-feedback loop involving importins, and initiates a transcriptional cascade that drives mitosis and cytokinesis. An engineered nuclear-restricted MYB3R4 mimics the cytokinin effects in enhancement of cell proliferation and meristem growth.

One Sentence Summary:

[*]Correspondence to: meyerow@caltech.edu; henrik.jonsson@slcu.cam.ac.uk.
[#]Present Address: National Key Laboratory of Plant Molecular Genetics, CAS Center for Excellence in Molecular Plant Sciences, Chinese Academy of Sciences, and CAS-JIC Center of Excellence for Plant and Microbial Sciences (CEPAMS), Shanghai 200032, China
[†]Present Address: BPMP, Univ Montpellier, CNRS, INRAE, Institut Agro, Montpellier, France.

Author contributions: W.Y. and E.M.M. initiated and designed the study; W.Y., S.C., P.R., K.S., A.G., and R.W. performed experiments; N.K. and H.J. performed modelling and simulation; A.G. analyzed the RNA FISH data; W.Y. and E.M.M. wrote the manuscript. All authors discussed and commented on the manuscript.

Competing interests: Authors declare no competing interests.

Data and materials availability: All data are available in the main text or the supplementary materials. Sequencing data are available at the NCBI Gene Expression Omnibus (GEO; https://www.ncbi.nlm.nih.gov/geo/) under accession number: GSE144049. Please contact E.M.M. for material requests.

Supplementary Materials:
Materials and Methods
Mathematical Modeling
Figures S1-S15
Tables S1-S4
Movies S1-S9
References (42–56)

Cytokinin promotes nuclear localization of a transcription factor to activate cell division.

Organ morphogenesis in plants is largely determined by the rate and patterns of cell division (1) occurring primarily in meristematic tissues such as the shoot and root meristems, and vascular cambium (2). The plant hormone cytokinin stimulates cell proliferation (3, 4) and acts with auxin to coordinate the balance between stem cell division and differentiation (5, 6). While the molecular mechanisms underlying plant cell cycle progression (7) and cytokinin signal transduction (8–11) have been well-characterized, it is unclear how cytokinin signals activate mitotic cell division.

The Arabidopsis shoot apical meristem (SAM) harbors stem cells that undergo active proliferation (12). Reduced cytokinin levels (13, 14) or impaired cytokinin signalling (15) result in smaller meristems with fewer cells. Exogenous cytokinin application promotes cell division, leading to enlarged meristems in wild-type (Col-0) plants that closely resemble those in the cytokinin oxidase mutant *ckx3 ckx5* (16) in which endogenous cytokinin levels are elevated due to reduction in cytokinin degradation (fig. S1).

Two MYB3R transcription factors regulate cytokinin response

A family of three-repeat R1R2R3 MYB transcription factors have been implicated in the control of mitotic gene expression (17–20). Among the five *MYB3R* genes in Arabidopsis, only *MYB3R1* and *MYB3R4* are highly expressed in the SAM, and their mRNAs are enriched in dividing cells, as assayed by *in situ* hybridization (fig. S2A). Compared to wild type, the *myb3r1 myb3r4* double mutant (20) has a reduced number of cells in both the shoot and root meristems (Fig. 1, A and C, and fig. S3). After cytokinin treatment, a large proportion (~60–70%) of *myb3r1 myb3r4* SAMs terminated prematurely (fig. S2, B to F). In *myb3r1 myb3r4* SAMs that did not terminate, the meristem size decreased and the number of the epidermal (L1) cells was reduced from 164 ±19 (n=11) in mock-treated controls to 109 ± 39 (n=11) after 100 μM BA treatment (3 external applications spaced by 2 days), whereas in wild-type SAMs the same cytokinin treatment increased the number of L1 cells from 269 ± 15 (n=12) to 378 ± 24 (n=11) (Fig. 1, B and C). Therefore, instead of sustaining cell proliferation activity, high levels of cytokinin increase the relative ratio of stem cell differentiation to division in a *myb3r1 myb3r4* genetic background, suggesting that cytokinin-activated cell division in the shoot meristem requires MYB3R1 and/or MYB3R4.

MYB3R1 and MYB3R4 activate core cell cycle gene expression

Genomic binding targets of MYB3R1 and MYB3R4 were identified using chromatin immunoprecipitation sequencing (ChIP-seq). Because expression of *MYB3R1* and *MYB3R4* is restricted to dividing cells (fig. S2A), and because of the low stability of these proteins (21), we applied the Maximized Objects for Better Enrichment (MOBE)-ChIP method, a strategy designed to detect low signals (22). We dissected and pooled approximately 1,000 shoot meristems from *pMYB3R1::GFP-MYB3R1* and *pMYB3R4::GFP-MYB3R4* plants. MYB3R1 and MYB3R4-bound DNA fragments were purified using an anti-GFP antibody and sequenced. From three biological replicates (i.e. ~3,000 meristems for each MYB3R protein), we identified 5,477 and 171 gene regions that

were bound by MYB3R1 and MYB3R4, respectively (Table S1). 97% of the MYB3R4 targets were shared by MYB3R1 (Fig. 2A); their binding regions also largely overlapped at the gene promoters (fig. S4A). Compared to wild type, the expression levels of the 166 MYB3R1 and MYB3R4 common target genes were mildly increased in *myb3r1* inflorescence meristems while most were down-regulated in the *myb3r4* single or the *myb3r1 myb3r4* double mutants (Fig. 2B, and fig. S4, B and C). Thus MYB3R4 predominantly activates gene expression, consistent with a dual luciferase assay showing that the promoter activity of target genes was enhanced markedly by MYB3R4 (fig. S4D). The overlap of MYB3R1 and MYB3R4 targets and their proximity when bound at gene promoters suggest the possibility of cooperative action in transcriptional control, as for MYB3R1 interacting with MYB3R3 and MYB3R5 in inhibition of cell division in post-mitotic or DNA-damaged cells (21, 23–25), and with TSO1 in regulation of flower morphogenesis (26). Indeed, through bimolecular fluorescence complementation (BiFC) and co-immunoprecipitation (CoIP) assays, it was found that MYB3R1 associates with MYB3R4 (fig. S5).

In synchronized *Arabidopsis* tissue culture cells (27), the expression levels of most MYB3R1 target genes remain constant during the cell cycle (fig. S6A), in line with their broad roles in developmental and metabolic processes (fig. S6B). In contrast, MYB3R4 targets exhibited a sharp increase in RNA expression at the G2/M transition (fig. S6, A and C). RNA FISH for 19 tested targets detected their mRNAs only in dividing cells (Fig. 2C, and fig. S6, D and E). MYB3R1 and MYB3R4 targets are involved in all key steps of mitotic progression such as cyclin-dependent kinase (CDK) activation/inhibition, chromosome re-organization/segregation, and assembly of the phragmoplast structure (Fig. 2D). We previously showed that the mRNAs of *CELL DIVISION CYCLE 20* (*CDC20*) and *CELL CYCLE SWITCH 52B* (*CCS52B*), encoding coactivators of the anaphase-promoting complex/cyclosome (APC/C) that targets cell cycle proteins for degradation (28), are expressed in dividing cells but sequestered in the nucleus before nuclear envelope breakdown (NEBD) (29). Both *CDC20* and *CCS52B* are direct binding targets of MYB3R1 and MYB3R4. We also observed enrichment of genes that modulate transcription, signal transduction, cell wall synthesis/modification, and cell wall signalling (Fig. 2D; Table S2).

Nucleo-cytoplasmic dynamics of MYB3R4 during cell division

Both GFP-MYB3R1 and GFP-MYB3R4 fusion proteins are functional in genetic complementation assays (fig. S7A). Similarly to typical transcription factors, GFP-MYB3R1 is localized in the nucleus (fig. S7B, and movie S1). For MYB3R4, exclusive nuclear localization is only seen in a small proportion (~ 6%) of cells while in a majority of GFP-MYB3R4 expressing cells, GFP fluorescence is present in both cytoplasm and nucleus (Fig. 2E, and fig. S7C, and movies S2, S3). This is the case in both shoot and root meristem cells (fig. S8, A and B) as well as in non-dividing cells in which GFP-MYB3R4 is ectopically expressed from the Arabidopsis *UBIQUITIN10* (*UBQ10*) promoter (fig. S8, C and D). Leptomycin B (LMB) treatment, which blocks nuclear export (30), results in re-distribution of GFP fluorescence signals into the nucleus (fig. S8A, and movies S4), demonstrating that MYB3R4 is a nuclear-exported transcription factor.

Time lapse observations of individual cells undergoing division revealed a recurrent pattern of rapid changes in GFP-MYB3R4 protein localization (Fig. 2F, and fig. S9). Preceding cell division, GFP-MYB3R4 fluorescence signal was detected predominantly in the cytoplasm. At the onset of mitosis, shortly before NEBD, a rapid nuclear accumulation of GFP-MYB3R4 led to the highest nuclear concentration of the protein observed in the cell cycle. During the subsequent steps of mitotic division, GFP-MYB3R4 was enriched in the cellular domains corresponding to spindles and phragmoplast. After nuclear envelope reformation at the end of cytokinesis, GFP-MYB3R4 protein showed a second phase of nuclear accumulation, but was soon exported back to the cytoplasm. Constitutively expressed GFP-MYB3R4 also exhibits transient nuclear localization in prophase cells (fig. S8C).

Cytokinin promotes MYB3R4 nuclear shuttling

To characterize the factors that regulate MYB3R4 nucleo-cytoplasmic trafficking, we first changed photosynthetic activity (light/dark shift) or nutrient status, both of which affect cell division (31). Light slightly increased the nuclear proportion of MYB3R4, while the other changes had no effect (fig. S10). Because MYB3R4 is required for cytokinin-activated cell division, we next tested whether cytokinin modulates MYB3R4 subcellular dynamics. A series of different concentrations of trans-zeatin (tZ), the most prevalent cytokinin in plants, was applied to the *GFP-MYB3R4* SAMs. High concentrations of tZ (≥100 μM) lead to re-localization of GFP-MYB3R4 into the nucleus in all of the cells where the protein was present (Fig. 3A, and fig. S11, A and B). Similar effects were observed for isopentenyladenine (iP) and BA (Fig. 3A, and movies S5–S7), but auxin had no effect (fig. S11C). Cytokinin action on MYB3R4 nuclear accumulation was not inhibited by cycloheximide (CHX, a protein synthesis inhibitor) (fig. S11D), indicating the movement of pre-existing MYB3R4 protein into the nucleus, and that MYB3R4 nuclear trafficking is a direct response to cytokinin.

To dissect how cytokinin promotes MYB3R4 nuclear localization, we analyzed the expression patterns of all importin and exportin genes (32) at the shoot apex. Most display a uniform distribution or are partially enriched in flower primordia. However, the mRNAs of *IMPORTIN ALPHA 3* (*IMPA3*), encoding the importin subunit α−3 also known as *MOS6* (*MODIFIER OF SNC1, 6*) (33), and *IMPA6*, exhibit a patchy pattern resembling the expression of cell cycle-regulated genes (Fig. 3B, and fig. S12). We confirmed their expression in dividing cells by RNA FISH (fig. S13, A and B), and by fluorescence reporter live imaging (fig. S13C). Both *IMPA3* and *IMPA6* were direct targets of MYB3R1 and MYB3R4 in the ChIP-seq experiments (fig. S13D). IMPA3 and IMPA6 are α family importins that function as adaptors to recognize target proteins for nuclear import. To examine the possible impact of importins on MYB3R4 nuclear translocation, we co-expressed RFP-IMPA3 and GFP-MYB3R4 in *Nicotiana benthamiana* leaf cells. In the absence of RFP-IMPA3, GFP-MYB3R4 shows a nuclear and cytoplasmic distribution similar to that in Arabidopsis cells. After co-expression with RFP-IMPA3, the nuclear proportion of GFP-MYB3R4 protein was significantly increased (Fig. 3C). In contrast, in the Arabidopsis *impa3–1* and *impa6–2* mutant SAMs, the relative amount of GFP-MYB3R4 in the nucleus was reduced compared to the wild-type plants (fig. S13, E and F). Therefore, it seems likely that MYB3R1 and MYB3R4 activate *IMPA3* and *IMPA6* expression,

facilitating MYB3R4 nuclear importation. This interplay between MYB3R4 and importins could represent a positive feedback loop that would enable more rapid nuclear import of MYB3R4 proteins. To test the feasibility of this hypothesis, we established a mathematical model to simulate MYB3R4 dynamics during the cell cycle. When using experimentally derived parameter values, we found that a peak of cytokinin input induces nuclear translocation of MYB3R4 (fig. S14, A–D). Incorporating the positive feedback with IMPA3 and IMPA6 causes MYB3R4 nuclear trafficking to become both faster and stronger (fig. S14, E–G).

The level of cytokinins, like the expression of mitotic genes, fluctuates during the plant cell cycle: endogenous cytokinin content slightly increases in the middle of S phase and exhibits a sharp peak at the G2/M transition (34–36). The first peak of cytokinins is in line with the report that cytokinin induces *CYCLIN D3* (*CYCD3*) expression for the G1/S transition (37). It has also been shown that inhibiting cytokinin synthesis at G2 blocks mitotic entry in tobacco Bright Yellow 2 (BY-2) cells (38). Our data demonstrate that i) the second peak of cytokinin levels coincides with rapid MYB3R4 nuclear accumulation, and ii) cytokinin promotes MYB3R4 nuclear re-localization but requires high hormone concentration. On the basis of these observations, we postulate that the high concentration of cytokinins at the G2/M transition promotes MYB3R4 nuclear localization to activate mitotic cell cycle gene expression (Fig. 3D).

MYB3R4 constitutive nuclear localization mimics cytokinin response

Finally, we tested whether perturbing MYB3R4 nucleo-cytoplasmic shuttling would influence cell division activity. To localize a nuclear export signal (NES), we generated a series of 11 truncated GFP-tagged MYB3R4 derivatives, and expressed them in a wild-type background under control of the *MYB3R4* promoter (fig. S15A). Subcellular localization analysis identified a sequence within the MYB3R4 carboxy-terminal region that is necessary and sufficient for cytosolic targeting (fig. S15B, and movie S8). Sequence comparison between MYB3R4 orthologues in different plant species identified a conserved sequence that could act as an NES (Fig. 4A). When the Phe (F) and Leu (L) residues were simultaneously mutated to Ala (A), nuclear export was abolished and the GFP-MYB3R4^{mNES} protein was exclusively nuclear (Fig. 4B, and movie S9).

GFP-MYB3R4^{mNES} shows transcriptional activity (fig. S15C) and exhibits a similar DNA binding profile as the natural GFP-MYB3R4 (fig. S15D). Transcriptomic analysis showed an opposite trend in the *pMYB3R4::GFP-MYB3R4*^{mNES} meristems compared to the *myb3r4* mutant, with the expression of most MYB3R4 target genes greatly upregulated (fig. S15E). RNA FISH showed that in *pMYB3R4::GFP-MYB3R4*^{mNES} the number of cells expressing MYB3R4 targets such as *CDC20* is increased (Fig. 4C). These plants showed enlarged SAMs (Fig. 4D) and expanded *WUSCHEL* (*WUS*) expression (Fig. 4E). These phenotypes resemble, although are weaker than, those of wild-type plants treated with cytokinin. Furthermore, the growth retardation phenotypes of cytokinin-deficient plants of genotype *35S::CKX1* (13) or of cytokinin receptor mutant plants of genotype *ahk2 ahk3* (15) could be rescued by *pMYB3R4::GFP-MYB3R4*^{mNES} (fig. S15, F and G). Thus, by

engineering a constitutively nuclear-localized form of MYB3R4, we were able to partially recapitulate cytokinin action.

Discussion

Underlying the many aspects of cytokinin-regulated developmental and physiological processes (11, 39) is the fundamental role of cytokinin in stimulating cell proliferation. Here we report that cytokinin directly promotes MYB3R4 nuclear localization to activate mitosis. Our data, together with that on cytokinin-induced *CYCD3* expression (37), have revealed a mechanistic framework underlying cytokinin-regulated cell division. The dual regulatory modes of cytokinin in *CYCD3* transcription and MYB3R4 nucleo-cytoplasmic shuttling ensure precise control of cell cycle transitions in response to different levels of cytokinin input, consistent with the dose-dependent action of cytokinin in plant cell division (4). Cytokinin-triggered MYB3R4-IMPA3/6 positive feedback leads to rapid MYB3R4 nuclear accumulation shortly before mitosis, but the transience of MYB3R4 presence in the nucleus is guaranteed by the dissolution of the nuclear membrane at prometaphase, which eliminates the possibilities of importin activity and nuclear localization. This allows for only one round of mitotic activation during the cell cycle. Variation of cytokinin levels in meristem cells, likely perceived by intracellular cytokinin receptors (40, 41), and acting through nuclear localization of a transcription factor, regulates stem cell numbers in the shoot stem cell niche.

Supplementary Material

Refer to Web version on PubMed Central for supplementary material.

Acknowledgments:

We thank M. Ito, Y. Helariutta, P. Tarr, H. Liu, and NASC for materials, J. Gruel for help with the computational modelling, K. Jaeger for assistance with DNA library preparation, G. Evans for assisting with the confocal microscopy analysis, D. Bergmann for helpful discussions.

Funding:

This work was supported by the Gatsby Charitable Foundation (GAT3395/DAA and GAT3395/PR4B) to E.M.M. and H.J. The laboratory of E.M.M. is supported by the Howard Hughes Medical Institute. R.W. had funding from Leverhulme Trust grant RPG-2015-285. The Microscopy Facility at the Sainsbury Laboratory is supported by the Gatsby Charitable Foundation.

References and Notes:

1. Meyerowitz EM (1997). Genetic control of cell division patterns in developing plants. Cell 88, 299–308. [PubMed: 9039256]
2. Greb T, Lohmann JU (2016). Plant stem cells. Curr. Biol 26, 816–821.
3. Miller CO, Skoog F, Von Saltza MH, Strong FM (1955). Kinetin, a cell division factor from deoxyribonucleic acid. J. Am. Chem. Soc 77, 1392–1392.
4. Schaller GE, Street IH, Kieber JJ (2014). Cytokinin and the cell cycle. Curr. Opin. Plant. Biol 21, 7–15. [PubMed: 24994531]
5. Schaller GE, Bishopp A, Kieber JJ (2015). The yin-yang of hormones: cytokinin and auxin interactions in plant development. Plant Cell 27, 44–63. [PubMed: 25604447]

6. Moubayidin L, Di Mambro R, Sabatini S (2009). Cytokinin–auxin crosstalk. Trends Plant Sci. 14, 557–562. [PubMed: 19734082]
7. De Veylder L, Beeckman T, Inzé D (2007). The ins and outs of the plant cell cycle. Nat. Rev. Mol. Cell Biol 8, 655–665. [PubMed: 17643126]
8. Mähönen AP, Bonke M, Kauppinen L, Riikonen M, Benfey PN, Helariutta Y (2000). A novel two-component hybrid molecule regulates vascular morphogenesis of the Arabidopsis root. Gene Dev. 14, 2938–2943. [PubMed: 11114883]
9. Inoue T, Higuchi M, Hashimoto Y, Seki M, Kobayashi M, Kato T, Tabata S, Shinozaki K, Kakimoto T (2001). Identification of CRE1 as a cytokinin receptor from Arabidopsis. Nature 409, 1060–1063. [PubMed: 11234017]
10. Hwang I, Sheen J (2001). Two-component circuitry in Arabidopsis cytokinin signal transduction. Nature 413, 383–389. [PubMed: 11574878]
11. Kieber JJ, Schaller GE (2018). Cytokinin signaling in plant development. Development 145, dev149344. [PubMed: 29487105]
12. Reddy GV, Heisler MG, Ehrhardt DW, Meyerowitz EM (2004). Real-time lineage analysis reveals oriented cell divisions associated with morphogenesis at the shoot apex of *Arabidopsis thaliana*. Development 131, 4225–4237. [PubMed: 15280208]
13. Werner T, Motyka V, Laucou V, Smets R, Van Onckelen H, Schmülling T (2003). Cytokinin-deficient transgenic Arabidopsis plants show multiple developmental alterations indicating opposite functions of cytokinins in the regulation of shoot and root meristem activity. Plant Cell 15, 2532–2550. [PubMed: 14555694]
14. Miyawaki K, Tarkowski P, Matsumoto-Kitano M, Kato T, Sato S, Tarkowska D, Tabata S, Sandberg G, Kakimoto T (2006). Roles of Arabidopsis ATP/ADP isopentenyltransferases and tRNA isopentenyltransferases in cytokinin biosynthesis. Proc. Natl Acad. Sci. USA 103, 16598–16603. [PubMed: 17062755]
15. Higuchi M, Pischke MS, Mähönen AP, Miyawaki K, Hashimoto Y, Seki M, Kobayashi M, Shinozaki K, Kato T, Tabata S, Helariutta Y Sussman M, Kakimoto T (2004). *In planta* functions of the Arabidopsis cytokinin receptor family. Proc. Natl Acad. Sci. USA 101, 8821–8826. [PubMed: 15166290]
16. Bartrina I, Otto E, Strnad M, Werner T, Schmülling T (2011). Cytokinin regulates the activity of reproductive meristems, flower organ size, ovule formation, and thus seed yield in *Arabidopsis thaliana*. Plant Cell 23, 69–80. [PubMed: 21224426]
17. Ito M (2005). Conservation and diversification of three-repeat Myb transcription factors in plants. J Plant Res. 118, 61–69. [PubMed: 15703854]
18. Umeda M, Aki SS, Takahashi N (2019). Gap 2 phase: making the fundamental decision to divide or not. Curr. Opin. Plant. Biol 51, 1–6. [PubMed: 30954849]
19. Haga N, Kato K, Murase M, Araki S, Kubo M, Demura T, Suzuki K, Müller I, Voß U, Jürgens G, Ito M (2007). R1R2R3-Myb proteins positively regulate cytokinesis through activation of KNOLLE transcription in *Arabidopsis thaliana*. Development 134, 1101–1110. [PubMed: 17287251]
20. Haga N, Kobayashi K, Suzuki T, Maeo K, Kubo M, Ohtani M, Mitsuda N, Demura T, Nakamura K, Jürgens G, Ito M (2011). Mutations in *MYB3R1* and *MYB3R4* cause pleiotropic developmental defects and preferential down-regulation of multiple G2/M-specific genes in Arabidopsis. Plant Physiol. 157, 706–717. [PubMed: 21862669]
21. Kobayashi K et al. (2015). Transcriptional repression by MYB3R proteins regulates plant organ growth. EMBO J. 34, 1992–2007. [PubMed: 26069325]
22. Lau OS, Davies KA, Chang J, Adrian J, Rowe MH, Ballenger CE, Bergmann DC (2014). Direct roles of SPEECHLESS in the specification of stomatal self-renewing cells. Science 345, 1605–1609. [PubMed: 25190717]
23. Chen P, Takatsuka H, Takahashi N, Kurata R, Fukao Y, Kobayashi K, Ito M, Umeda M (2017). Arabidopsis R1R2R3-Myb proteins are essential for inhibiting cell division in response to DNA damage. Nat. Commun 8, 1–12. [PubMed: 28232747]

24. Takahashi N, Ogita N, Takahashi T, Taniguchi S, Tanaka M, Seki M, Umeda M (2019). A regulatory module controlling stress-induced cell cycle arrest in Arabidopsis. eLife 8, e43944. [PubMed: 30944065]
25. Bourbousse C, Vegesna N, Law JA (2018). SOG1 activator and MYB3R repressors regulate a complex DNA damage network in Arabidopsis. Proc. Natl Acad. Sci. USA 115, E12453–E12462. [PubMed: 30541889]
26. Wang W, Sijacic P, Xu P, Lian H, Liu Z (2018). Arabidopsis TSO1 and MYB3R1 form a regulatory module to coordinate cell proliferation with differentiation in shoot and root. Proc. Natl Acad. Sci. USA 115, E3045–E3054. [PubMed: 29535223]
27. Menges M, De Jager SM, Gruissem W, Murray JA (2005). Global analysis of the core cell cycle regulators of Arabidopsis identifies novel genes, reveals multiple and highly specific profiles of expression and provides a coherent model for plant cell cycle control. Plant J. 41, 546–566. [PubMed: 15686519]
28. Yang W, Wightman R, Meyerowitz EM (2017). Cell cycle control by nuclear sequestration of *CDC20* and *CDH1* mRNA in plant stem cells. Mol. Cell 68, 1108–1119. [PubMed: 29225038]
29. Heyman J, De Veylder L (2012). The anaphase-promoting complex/cyclosome in control of plant development. Mol. Plant 5, 1182–1194. [PubMed: 23034505]
30. Fornerod M, Ohno M, Yoshida M, Mattaj IW (1997). CRM1 is an export receptor for leucine-rich nuclear export signals. Cell 90, 1051–1060. [PubMed: 9323133]
31. Jones AR, Forero-Vargas M, Withers SP, Smith RS, Traas J, Dewitte W, Murray JA (2017). Cell-size dependent progression of the cell cycle creates homeostasis and flexibility of plant cell size. Nat. Commun 8, 1–13. [PubMed: 28232747]
32. Meier I, Richards EJ, Evans DE (2017). Cell biology of the plant nucleus. Annu. Rev. Plant Biol 68, 139–172. [PubMed: 28226231]
33. Palma K, Zhang Y, Li X (2005). An importin α homolog, MOS6, plays an important role in plant innate immunity. Curr. Biol 15, 1129–1135. [PubMed: 15964279]
34. Nishinari N, Syōno K (1986). Induction of cell division synchrony and variation of cytokinin contents through the cell cycle in tobacco cultured cells. Plant Cell Physiol. 27, 147–153.
35. Redig P, Shaul O, Inzé D, Van Montagu M, Van Onckelen H (1996). Levels of endogenous cytokinins, indole-3-acetic acid and abscisic acid during the cell cycle of synchronized tobacco BY-2 cells. FEBS Lett. 391, 175–180. [PubMed: 8706911]
36. Dobrev P, Motyka V, Gaudinová A, Malbeck J, Trávníčková A, Kamínek M, Vaňková R (2002). Transient accumulation of *cis*-and *trans*-zeatin type cytokinins and its relation to cytokinin oxidase activity during cell cycle of synchronized tobacco BY-2 cells. Plant Physiol. Biochem 40, 333–337.
37. Riou-Khamlichi C, Huntley R, Jacqmard A, Murray JA (1999). Cytokinin activation of Arabidopsis cell division through a D-type cyclin. Science 283, 1541–1544. [PubMed: 10066178]
38. Laureys F, Dewitte W, Witters E, Van Montagu M, Inzé D and Van Onckelen H (1998). Zeatin is indispensable for the G2-M transition in tobacco BY-2 cells. FEBS Lett. 426, 29–32. [PubMed: 9598972]
39. Wybouw B, De Rybel B (2019). Cytokinin–a developing story. Trends Plant Sci. 24, 177–185. [PubMed: 30446307]
40. Wulfetange K, Lomin SN, Romanov GA, Stolz A, Heyl A, Schmülling T (2011). The cytokinin receptors of Arabidopsis are located mainly to the endoplasmic reticulum. Plant Physiol. 156, 1808–1818. [PubMed: 21709172]
41. Caesar K, Thamm AM, Witthöft J, Elgass K, Huppenberger P, Grefen C, Horak J, Harter K (2011). Evidence for the localization of the Arabidopsis cytokinin receptors AHK3 and AHK4 in the endoplasmic reticulum. J. Exp. Bot 62, 5571–5580. [PubMed: 21841169]
42. de Reuille PB et al. MorphoGraphX: A platform for quantifying morphogenesis in 4D. eLlife 4, e05864 (2015).
43. Lindsay DL, Sawhney VK, Bonham-Smith PC (2006). Cytokinin-induced changes in *CLAVATA1* and *WUSCHEL* expression temporally coincide with altered floral development in Arabidopsis. Plant Sci. 170, 1111–1117.

44. Yang W, Schuster C, Prunet N, Dong Q, Landrein B, Wightman R, Meyerowitz EM (2020). Visualization of protein coding, long non-coding and nuclear RNAs by FISH in sections of shoot apical meristems and developing flowers. Plant Physiol. 182, 147–158. [PubMed: 31722974]
45. Gendrel AV, Lippman Z, Yordan C, Colot V, Martienssen RA (2002). Dependence of heterochromatic histone H3 methylation patterns on the Arabidopsis gene *DDM1*. Science 297, 1871–1873. [PubMed: 12077425]
46. Blecher-Gonen R, Barnett-Itzhaki Z, Jaitin D, Amann-Zalcenstein D, Lara-Astiaso D, Amit I (2013). High-throughput chromatin immunoprecipitation for genome-wide mapping of in vivo protein-DNA interactions and epigenomic states. Nat. Protoc 8, 539. [PubMed: 23429716]
47. Langmead B, Trapnell C, Pop M, Salzberg SL (2009). Ultrafast and memory-efficient alignment of short DNA sequences to the human genome. Genome Bio. 10, R25. [PubMed: 19261174]
48. Zhang Y, Liu T, Meyer CA, Eeckhoute J, Johnson DS, Bernstein BE, Nussbaum C, Myers RM, Brown M, Li W, Liu XS (2008). Model-based Analysis of ChIP-Seq (MACS). Genome Biol. 9, R137. [PubMed: 18798982]
49. Bailey TL, Boden M, Buske FA, Frith M, Grant CE, Clementi L, Ren J, Li WW and Noble WS (2009). MEME SUITE: tools for motif discovery and searching. Nucleic Acids Res. 37, W202–W208. [PubMed: 19458158]
50. Huang W, Loganantharaj R, Schroeder B, Fargo D, Li L (2013). Pavis: a tool for peak annotation and visualization. Bioinformatics 29, 3097–3099. [PubMed: 24008416]
51. Robinson JT, Thorvaldsdóttir H, Winckler W, Guttman M, Lander ES, Getz G, Mesirov JP (2011). Integrative genomics viewer. Nat. Biotechnol 29, 24–26. [PubMed: 21221095]
52. Ramírez F, Dündar F, Diehl S, Grüning BA, Manke T (2014). deepTools: a flexible platform for exploring deep-sequencing data. Nucleic Acids Res. 42, W187–W191. [PubMed: 24799436]
53. Ramírez F, Ryan DP, Grüning B, Bhardwaj V, Kilpert F, Richter AS, Heyne S, Dündar F, Manke T (2016). deepTools2: a next generation web server for deep-sequencing data analysis. Nucleic Acids Res. 44, W160–W165. [PubMed: 27079975]
54. Patro R, Duggal G, Love MI, Irizarry RA, Kingsford C (2017). Salmon provides fast and bias-aware quantification of transcript expression. Nat. Methods 14, 417. [PubMed: 28263959]
55. Ge SX, Jung D, Yao R (2020). ShinyGO: a graphical gene-set enrichment tool for animals and plants. Bioinformatics 36, 2628–2629. [PubMed: 31882993]
56. Hellens RP, Allan AC, Friel EN, Bolitho K, Grafton K, Templeton MD, Karunairetnam S, Gleave AP, Laing WA (2005). Transient expression vectors for functional genomics, quantification of promoter activity and RNA silencing in plants. Plant Methods 1, 13. [PubMed: 16359558]

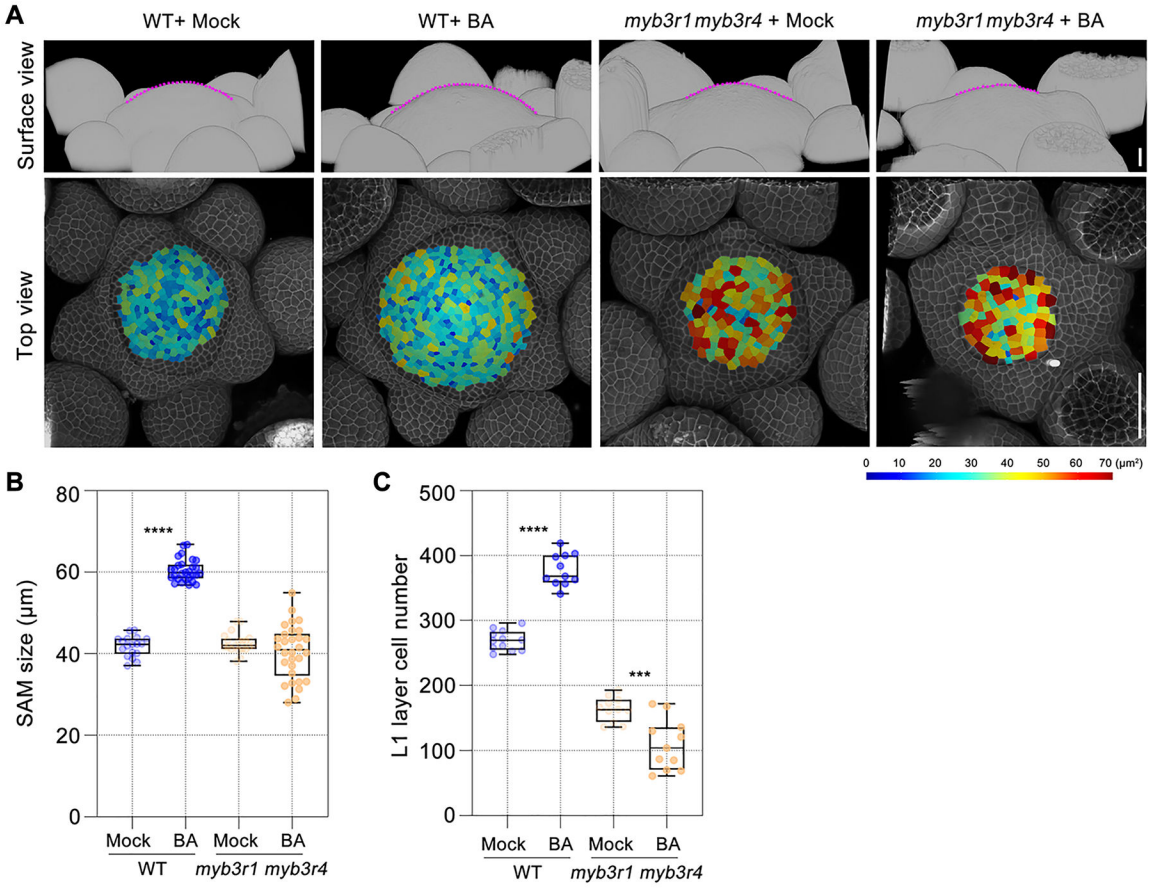

Fig. 1. A pair of MYB3R transcription factors regulate cytokinin-activated cell division in the *Arabidopsis* shoot meristem.

(A) The morphologies of wild-type (WT, Col-0) and *myb3r1 myb3r4* shoot apical meristems (SAMs) in response to cytokinin treatment. The shoot apices collected shortly after bolting (with stem length 1cm) were treated with BA (100 μM) three times at two-day intervals. The SAMs (top panels) are outlined with dashed lines (in magenta), they are surrounded by developing flower primordia. Bottom panels show segmented L1 (epidermal) cells. The cell walls were stained using propidium iodide (PI, shown in gray). Scale bar in top panel, 20 μm; in bottom panel, 50 μm.

(B and C) The effect of cytokinin treatment on meristem size (B) and cell number (C) in wild-type and *myb3r1 myb3r4* SAMs. ***P < 0.001, ****P < 0.0001 (two-tailed t-test).

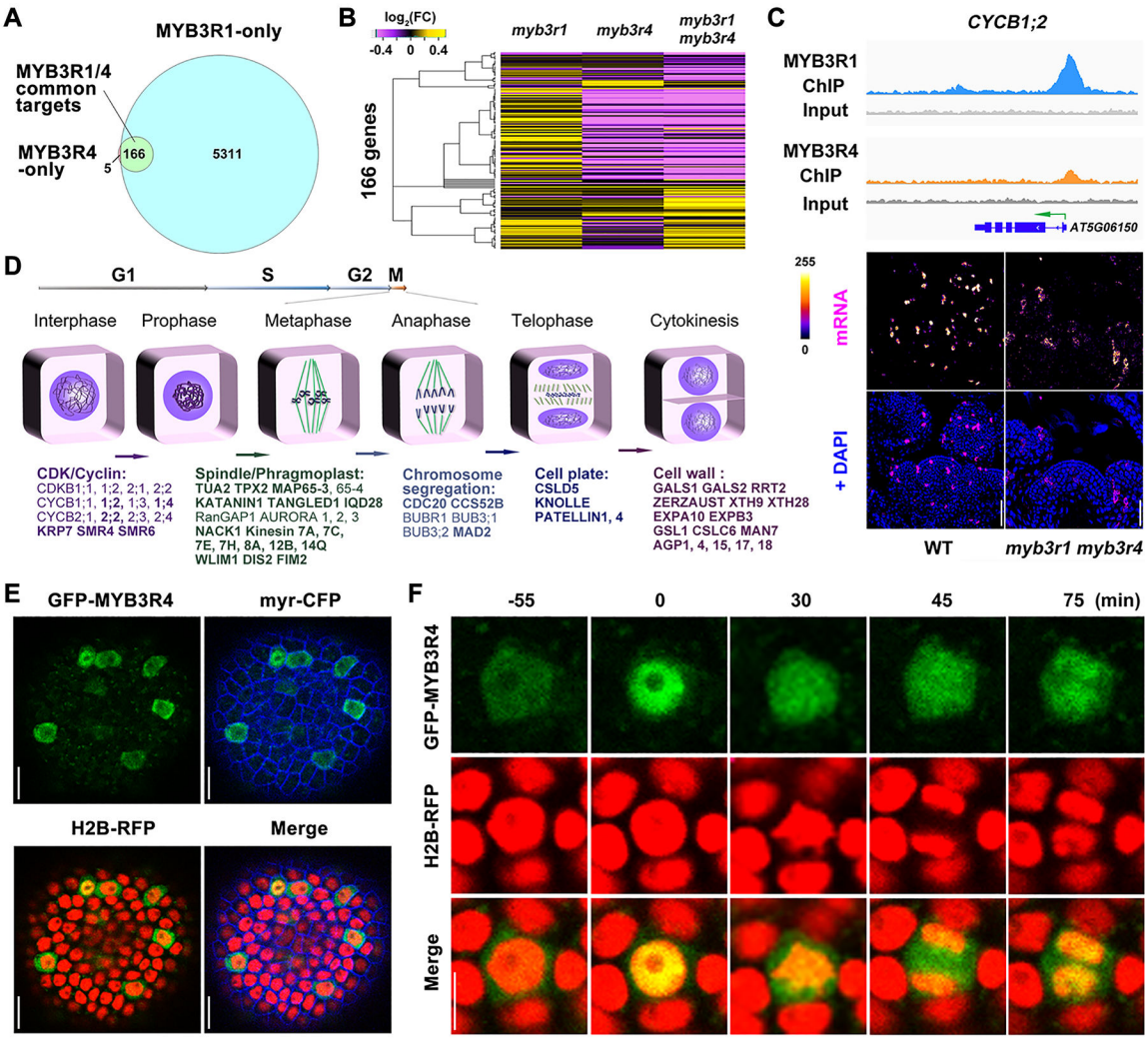

Fig. 2. MYB3R4 transiently localizes in the nucleus to activate the expression of mitotic cell cycle genes.

(A) Venn diagram showing the number of gene regions bound by MYB3R1 and MYB3R4 as detected by ChIP-seq.

(B) Hierarchical clustering of 166 MYB3R1 and MYB3R4 common target genes based on their relative expression levels, as detected by RNA-seq in shoot apices of single and double mutants compared to wild type. Yellow indicates increased expression and purple indicates decreased expression.

(C) MYB3R1 and MYB3R4 bind to target gene promoters and activate their expression in dividing cells. The top panels show genome browser tracks of MYB3R1 and MYB3R4 ChIP-seq coverage at a representative target gene *CYCB1;2*. The bottom panels show *CYCB1;2* expression in wild-type and *myb3r1 myb3r4* SAMs as revealed by RNA fluorescence *in situ* hybridisation (FISH). FISH signals are displayed using the Fire lookup table of Fiji (ImageJ) software. Scale bars, 50 μm.

(D) Classification of MYB3R1 and MYB3R4 targets based on their molecular functions. MYB3R1- and MYB3R4-regulated genes are involved in all key steps of mitotic progression. The common targets are shown in bold text.

(E) Nucleo-cytoplasmic shuttling of MYB3R4. Shown are SAM cells expressing GFP-MYB3R4 (green) together with a plasma membrane marker myr-CFP (blue) and a nuclear reporter H2B-RFP (red). Scale bars, 20 μm.

(F) The dynamic localization of GFP-MYB3R4 protein during cell division. MYB3R4 shows rapid translocalization from the cytoplasm to the nucleus at the onset of mitosis (time zero). Scale bar, 5 μm.

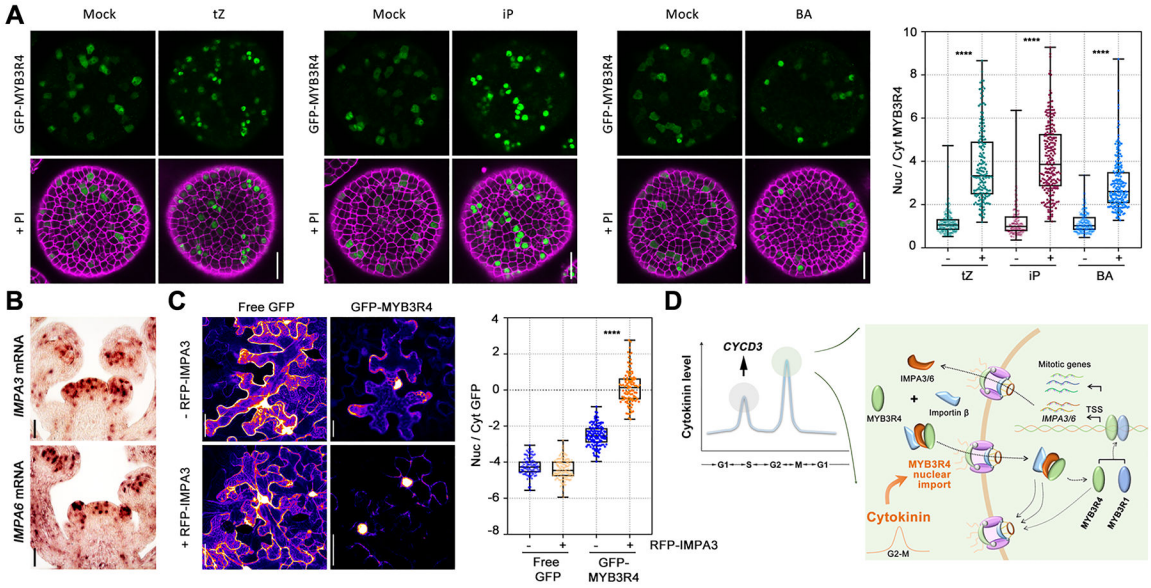

Fig. 3. Cytokinins promote MYB3R4 nuclear localization.

(A) The subcellular localization patterns of GFP-MYB3R4 after mock treatment or cytokinin treatment. GFP-MYB3R4 protein was predominantly nuclear after 6 h of 100 μM cytokinin treatment. The nuclear (nuc)-to-cytoplasmic (cyt) ratio of MYB3R4 was measured by quantifying the GFP fluorescence intensities in Fiji. Scale bars, 20 μm. ****P < 0.0001 (two-tailed t-test).

(B) The expression of MYB3R1 and MYB3R4 target genes *IMPA3* and *IMPA6* in dividing cells of the SAM. *IMPA3* and *IMPA6* mRNAs were detected by *in situ* hybridisation. Scale bars, 50 μm.

(C) IMPA3 facilitates MYB3R4 nuclear import. GFP-MYB3R4 was expressed in the absence (upper panel) or presence (lower panel) of RFP-IMPA3 in the tobacco leaf cells. Free GFP serves as a control. The Arabidopsis *UBQ10* promoter was used for expression of all genes. Scale bars, 50 μm. ****P < 0.0001 (two-tailed t-test).

(D) A schematic illustration of cytokinin-activated cell division and the feedback between importin and MYB3R4. A relatively high level of cytokinin induces *CYCD3* expression to promote G1/S transition (37). As cell cycle proceeds, a further increase in cytokinin abundance promotes MYB3R4 nuclear translocation. Inside the nucleus, MYB3R4 interacts with MYB3R1 to activate the expression of mitotic cell cycle genes as well as *IMPA3* and *IMPA6*. IMPA3 and IMPA6 subsequently facilitate MYB3R4 nuclear import, thus generating a positive feedback loop.

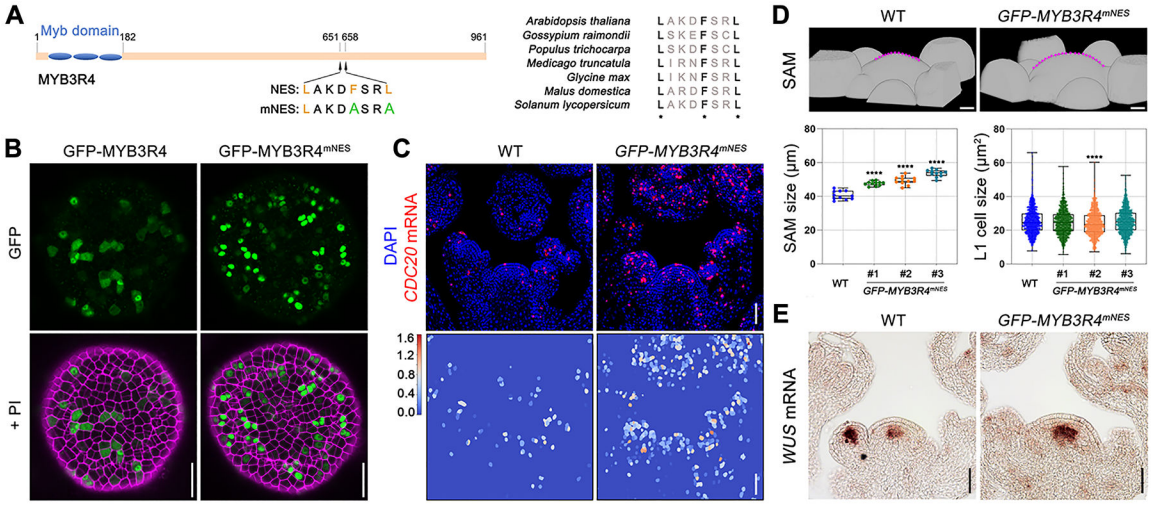

Fig. 4. MYB3R4 nuclear localization stimulates cell division and meristem growth.

(A) Analysis of MYB3R4 nuclear export signal (NES). The conserved hydrophobic residues of MYB3R4 NES are substituted with alanine in the mutated NES (mNES).

(B) Protein localisation of GFP-MYB3R4 and GFP-MYB3R4^{mNES} expressed under *MYB3R4* promoter. GFP-MYB3R4^{mNES} protein could be detected only in the nucleus. Scale bars, 20 μm.

(C) Increased expression of the target gene *CDC20* in wild type and *pMYB3R4::GFP-MYB3R4^{mNES}*. Bottom panels show heatmap of the segmented *CDC20* RNA FISH signals. Scale bars, 50 μm.

(D) Enhanced meristem growth in *pMYB3R4::GFP-MYB3R4^{mNES}*. Top panels are 3-D surface views of wild-type and *pMYB3R4::GFP-MYB3R4^{mNES}* SAMs. The SAMs are outlined with dashed lines (in magenta). Three representative *pMYB3R4::GFP-MYB3R4^{mNES}* transgenic lines were used for quantification of meristem size and L1 cell size. Scale bars, 20 μm. ****P < 0.0001 (two-tailed t-test).

(E) Comparison of *WUS* expression in wild-type and *pMYB3R4::GFP-MYB3R4^{mNES}* SAMs, as revealed by mRNA *in situ* hybridisation. Scale bars, 50 μm.